



HAL
open science

Assessment of clogging of managed aquifer recharge in a semi-arid region

Mohammed Zaidi, Nasre-Dine Ahfir, Abdellah Alem, Bouabid El Mansouri, Huaqing Wang, Said Taibi, Benoît Duchemin, Abdesselam Merzouk

► To cite this version:

Mohammed Zaidi, Nasre-Dine Ahfir, Abdellah Alem, Bouabid El Mansouri, Huaqing Wang, et al.. Assessment of clogging of managed aquifer recharge in a semi-arid region. *Science of the Total Environment*, 2020, 730, pp.139107. 10.1016/j.scitotenv.2020.139107 . hal-03490276

HAL Id: hal-03490276

<https://hal.science/hal-03490276>

Submitted on 20 May 2022

HAL is a multi-disciplinary open access archive for the deposit and dissemination of scientific research documents, whether they are published or not. The documents may come from teaching and research institutions in France or abroad, or from public or private research centers.

L'archive ouverte pluridisciplinaire **HAL**, est destinée au dépôt et à la diffusion de documents scientifiques de niveau recherche, publiés ou non, émanant des établissements d'enseignement et de recherche français ou étrangers, des laboratoires publics ou privés.



Distributed under a Creative Commons Attribution - NonCommercial 4.0 International License

Assessment of Clogging of Managed Aquifer Recharge in a Semi-Arid Region

Mohammed ZAIDI^{1, 2}, Nasre-Dine AHFIR^{1*}, Abdellah ALEM¹, Bouabid EL MANSOURI², Huaqing WANG¹, Said TAIBI¹, Benoît DUCHEMIN¹, Abdesselam MERZOUK²

¹Normandie Univ., UNIHAVRE, UMR 6294 CNRS, LOMC, 76600 Le Havre, France.

²Laboratory of Geosciences of Natural Resources, Hydroinformatic section, Faculty of Sciences, Ibn Tofail University, Maamora Campus, BP.133, 14000 Kénitra, Morocco.

*Corresponding Author: Nasre-Dine AHFIR (ahfirm@univ-lehavre.fr)

Normandie Univ, UNIHAVRE, UMR 6294 CNRS, LOMC, 76600 Le Havre, France.

Phone number: +33 (0) 235-217-117, fax number: +33 (0) 235-217-198

1 Assessment of Clogging of Managed Aquifer Recharge in a Semi-Arid

2 Region

4 Abstract

5 To overcome water scarcity issues in arid and semi-arid regions, Managed Aquifer Recharge
6 (MAR) remains a viable and suitable solution to manage and restore aquifers. However,
7 clogging represents a major issue that can affect the durability and efficiency of MAR
8 structures. The aim of this study was to evaluate the extent of clogging in MAR sites
9 (Berrechid, Morocco). To achieve this objective, two field-based studies were undertaken: the
10 first one consists of implantation of sand-filled columns in the recharge sites to evaluate the
11 surface and subsurface clogging. The second one consists of the implantation of pickets over a
12 750 m² area in each recharge site to measure the extent of deposit thickness on the surface of
13 the wadi bed. Results show that, despite the low rainfall (less than 1.4 mm/day) and the short
14 period (91 days) of the study, the deposits thickness exceeds 3 cm in a large part of the MAR.
15 The suspended solids concentrations measured in recharge sites ranged from 1.1 to 1.4 g/L.
16 Due to the particles retention, the estimation of the saturated hydraulic conductivity (k) of the
17 sand declines over 90% in the immediate entrance of the columns. The k values measured *in*
18 *situ* during the drying period ranged from 10⁻⁵ to 10⁻⁶ m/s. The k values of the cake formed,
19 without cracks, was about 10⁻⁸ m/s. The presence of cracks drives the entire infiltration.
20 However, due to the high plasticity index of the MAR soil, a slight reduction of cracks
21 opening during wetting cycles is observed. In addition, particles deposited in these cracks,
22 would contribute actively to the reduction of infiltration. The results of this study clearly
23 showed the MAR sites vulnerability in semi-arid regions due to physical clogging.

24 **Keywords:** semi-arid region; Managed Aquifer Recharge; particles transfer; hydraulic
25 conductivity; clogging; soil cracks

26 **Introduction**

27 In water-limited environments, population growth has led to amplified water demand
28 stressing aquifers and streams (Treese et al., 2009). Arid and semi-arid climates are
29 particularly susceptible, often relying on groundwater to support the needs of large urban
30 centres or irrigated agriculture in the absence of sufficient surface water resources
31 (Famiglietti, 2014). Also, natural recharge is intrinsically limited in these climates, and the
32 predicted effects of climate change on recharge in these regions are highly uncertain (Taylor
33 et al., 2012). In order to increase the security of groundwater resources, managed aquifer
34 recharge (MAR) programs have been developed and implemented globally (Stefan and
35 Ansems, 2018). MAR is an engineering system that aims to increase groundwater supplies by
36 water injection (well) into aquifers and also by infiltration being carried out from large and
37 accessible surface structures (constructed basins, and perfectly dimensioned or natural wadi
38 beds) (Bouwer, 2002; Missimer et al., 2015). Other objectives of this technique include
39 reducing marine intrusions, storing water and improving surface water quality (Dillon, 2005;
40 Dillon et al., 2009). Managed aquifer recharge was the subject of several research studies that
41 addressed its various technical and economic aspects (Marino, 1975; Detay, 1995).

42 The soil infiltration rate decreased due to the high rate of sedimentation during flow
43 periods. The study of Hatch et al., (2010) of Pajaro River in California, showed that the
44 hydraulic conductivity of the streambed ranged from 10^{-6} to 10^{-4} m/s within the experimental
45 site, with lower hydraulic conductivity determined later in the dry season, as deposits were
46 accumulated on the streambed during periods of low flow. For the Danube River (Vienna),
47 Blaschke et al., (2003) reported a reduction of the seepage rate by about 40% to 60% over a
48 period of 4.5 years. The experiment conducted by Pholkern et al., (2015) at the Mae Rim site

49 (Thailand) indicates that during the 22-day period of the experiment, with channel flow (0.05
50 m/s) and turbidity (200-950 NTU), vertical hydraulic conductivity decreased significantly
51 from 5.6×10^{-6} to 7.3×10^{-7} m/s between 0 and 0.03 m in depth.

52 Clogging has long been an issue in managed aquifer recharge (Dillon et al., 2016). The
53 main operational challenge of infiltration systems is usually management of clogging, which
54 causes a decrease in permeability. As a consequence, the recharge rate decreases, leading to
55 the failure of managed recharge system (Jeong et al., 2018). A study conducted by Pavelic
56 and Dillon (1997) found that clogging was the dominant reason for abandonment of Aquifer
57 Storage and Recovery projects. Clogging of surface infiltration has multiple impacts,
58 counting: i) decreasing infiltration rates (Schubert, 2002) and ii) reducing soil infiltrability
59 efficiency, which involves a regular maintenance (Siegrist, 1987). In porous media, the
60 clogging layer (cake) is the part of the medium over which a sharp drop in hydraulic head
61 occurs as water infiltrates a sedimentary profile (Houston et al., 1999). There are two distinct
62 kinds of clogging layers that can be formed in the infiltration surface: i) a top layer consisting
63 of suspended particles material, algae and/or microbes accumulating above native material
64 and ii) a lower layer containing the autochthon sediment with organic and inorganic solids
65 trapped in the pore space (Hutchison et al., 2013).

66 Clogging can be the result of chemical, biological or physical mechanisms or some
67 combination of the three: (i) chemical clogging, which depends on chemical factors that
68 control the colloidal stability of the particles and minerals precipitated from water (Mays and
69 Hunt, 2007); (ii) biological by the growth of microorganisms (algae, biofilm and bacteria) at
70 the infiltration surface or on a thin layer (Nie et al., 2011) and (iii) physical or mechanical
71 related to solid particles inputs (Rinck-Pfeiffer et al., 2000; Siriwardene et al., 2007) and
72 environmental compaction related to basin activities, water loads when the basin is filled and
73 settling of sediment deposits themselves (Gonzalez-Merchan et al., 2012). In nature,

74 sediments carried by flows can have several origins but mainly erosion of crumbly geological
75 formations (Gaskin et al., 2003) or by human activities, such as the extractive industry (gravel
76 and clay extraction), agricultural activities and construction projects (Ryan, 1991). Hydraulic
77 conductivity is one of the most significant soil properties that controls water infiltration from
78 the surface to subsurface. The hydraulic conductivity is largely dependent on the soil
79 properties and can therefore vary considerably in space and time (Viviani and Iovino, 2004;
80 Sepaskhah and Sokoot, 2010;). For clayey soils, desiccation cracking is a phenomenon that
81 may considerably increase the hydraulic conductivity. However, as shown by Rayhani et al.
82 (2008), under cyclic drying and wetting, for some highly plastic soils, hydraulic conductivity
83 decreased with an increase in permeation time, which is attributed to the cracks self-healing.

84 Many studies have been undertaken to study the clogging phenomenon *in situ*.
85 Skolasińska (2006) identified the post-depositional changes that have occurred in river
86 deposits affected by forced infiltration of river water and concluded that the decomposition of
87 organic matter present in deposits or in infiltrating water is a very important factor controlling
88 clogging. Casas-Mulet et al. (2017) studied the main hydraulic factors and trends in fine
89 sediment accumulation on a river by installing sediment collectors in a lateral gravel bar
90 subject to irregular flow fluctuations in the river. They estimated that an important horizontal
91 inter-gravel transport contributed to a significant accumulation of fine sediments. Fetzer et al.
92 (2017) investigated the dynamics of clogging by comparing infiltration of silty fine particles
93 and sandy fine particles and by comparing the results between laboratory and field
94 experiments. They showed that clogging is rather pronounced in the field due to a highly
95 fluctuating water regime, a polydispersed suspension and a high concentration of suspended
96 particles in comparison to laboratory conditions.

97 In Morocco, the techniques of artificial recharge started since 1958 (Sadiki et al.,
98 2019). The first experiments were carried out on the Charf El Akab aquifer in the North-

99 Western area. Then these techniques were generalised to all unconfined aquifers that suffer
100 from excessive exploitation of groundwater resources. There were 40 projects carried out, of
101 which 96% are on the embankments constructed on streams, alimented by rainwater and dam
102 releases. The clogging of recharge areas represents the common issue between these projects,
103 induced by sediments mobilised during flows.

104 Until now and to our knowledge, there have been no studies on the clogging processes
105 in artificial recharge facilities in Morocco (semi-arid region) according to hydro-
106 meteorological conditions of the field. Thus, an investigation in that optic was carried out.
107 The aim of this study was to evaluate the extent of clogging in the field by measuring the
108 amount of fine particles infiltrating in depth and the thickness of sediments deposited on the
109 bed surface in recharge sites. This was accomplished by using an original approach that
110 consists of implanting pickets and sand-filled columns in recharge sites for assessing particle
111 deposition on the soil surface and subsurface. Saturated hydraulic conductivity measurements
112 were made, *in situ* and in the laboratory, to evaluate the effect of deposit accumulation on
113 infiltration. Deposited particles, in the surface and subsurface, characteristics (particles size
114 and composition of the organic and inorganic matter) were determined.

115

116 **1. Materials and Methods**

117 **1.1. Description of study area**

118 Berrechid Plain is located in the centre of Morocco (Fig. 1). It extends to 1,500 km².
119 This region is characterised by an arid to semi-arid climate, with an average temperature of
120 18°C. The annual average rainfall varies from 280 to 310 mm/year (El Assaoui et al., 2015).
121 The plain is marked by intense industrial activity, particularly the ceramics industry and the
122 development of agriculture based on the exploitation of groundwater resources. According to
123 the Bouregreg and Chaouia Hydraulic Basin Agency (ABHBC), the water balance deficit

124 increased from 20 Mm³ in 2010 to 30 Mm³/year in 2016, which was linked to withdrawals
125 from about 3,000 wells and boreholes, where 96% of the total volume pumped is for
126 agricultural use (Ouassissou et al., 2019). For many years, this aquifer has been the subject of
127 many geological and hydrogeological studies (Hazan and Moullard, 1962; Ruhard, 1975; El
128 Mansouri, 1993). Berrechid Plain takes the form of a subsidence basin in which Triassic,
129 Cretaceous, Pliocene and Quaternary geologic formations have been deposited on the
130 Paleozoic basement (Hazan and Moullard, 1962). The aquifer is supplied mainly by lateral
131 flows from the Phosphate Plateau in the southern part of the basin, mainly Boumoussa,
132 Tamedrost, Mazer and El Himmer (27 km length) wadies (Fig. 1) and by direct infiltration
133 from rainfall and the return of irrigation flow (El Ghali et al. 2020).

134 **Fig.1**

135 The surface deposits in the study area are generally dominated by aggregates topped
136 with silty red clay, gravel and cobble (El Mansouri, 1993). In the southern section of the
137 aquifer, El Himmer wadi has been equipped since 2008 by a managed aquifer recharge
138 (MAR) system: two percolation tanks (S1 and S3), which retard flood water to facilitate
139 infiltration of the underlying aquifer during runoff, as well as two recharge releases (S2 and
140 S4), which are used to retain dam's releases inducing slow drainage of water into the
141 streambed to ameliorate the infiltration rate (Cf. Fig. 1; photos a and b). Note that outside the
142 rainy period and dam's releases, El Himmer wadi remains dry. After more than ten years of
143 use and despite some curing operations carried out by the authorities to remove sediments
144 carried by the flows, a high volume of fine soils transported by flows each year settles along
145 the wadi, particularly in percolation basins, thereby limiting groundwater recharge.

146 **1.2. Rainfall**

147 The daily rainfall time series, provided by ABHBC, covering a period of eight months
148 (from August, 2018 to March 2019) is depicted in Fig. 2. Rainfall data was collected from El

149 Mers climate station (x=320,050 m; y=279,150 m) located at 10 km from the study area (Cf.
150 Fig. 1). The observation of the daily rainfall histogram (Fig. 2) distinguishes two typical
151 periods: one was from October to November with 151.8 mm, and another was relatively dry
152 between December and January with rainfall about 25.4 mm. During the study period (from
153 October 20th, 2018 to January 19th, 2019), the total rainfall was less than 122.6 mm, with an
154 average of 1.34 mm/day. The mean daily temperature was around 18°C (Fig. 2).

155 **Fig.2**

156 **1.3. Field investigations**

157 As mentioned above, the objective of this study was to assess the physical clogging in
158 MAR sites (S1, S2, S3, and S4) located along the El Himmer Wadi (Fig. 1). To achieve this
159 objective, at each studied site and over an area of 750 m² (15*50), pickets and sand-filled
160 columns were implanted in different positions (Fig. 3c). The implantation of these pickets and
161 columns was done on October 20th, 2018. More than 60 pickets have been implanted. The top
162 of each picket remained uncovered by 10 cm, which makes it possible to measure the
163 thickness of the deposits after 91 days of exposure to hydro-meteorological conditions (until
164 January 19th, 2019). The implanted PVC columns were 7.5 cm in inner diameter and 30 cm in
165 length. The sand filling the columns was sieved and cleaned to remove all organic matter and
166 fine particles attached to the grains. The grain-size distribution of the sieved sand ranged from
167 140 to 1,200 µm, with a mean diameter of 520 µm and a uniformity coefficient of 2.1. The
168 average porosity and saturated hydraulic conductivity of the sand filling columns were 0.38
169 (± 0.01) and $k = 2.2 \times 10^{-3}$ m/s ($\pm 2 \times 10^{-4}$), respectively. A total of 24 columns were buried
170 (Figs. 3b and c) in the four recharge sites. The top of each column was on the same level of
171 the wadi bed. The positions of the pickets and the columns were recorded by GPS. After 91
172 days of exposure to natural conditions of the field (from October 20, 2018 to January 19th,
173 2019), 12 columns and 43 pickets were recovered successfully, while the others were found

174 damaged. Notice that all implanted columns and pickets in site S4 were damaged. The
175 columns were dig up and carefully transported to the laboratory for treatment and analysed.
176 Each column was divided into 1 cm layers. For each layer, the quantity of fine particles
177 retained was determined by washing, drying and weighing (Alem et al., 2013). The particles
178 deposition profile along the length of each column was determined. The deposited particles
179 collected from sand during the washing process were stored in vials for granulometric
180 analysis in order to determine the particle size distribution, using a laser diffraction particle
181 size analyser.

182 **Fig.3**

183 In this study, saturated hydraulic conductivity measurements were performed in recharge sites
184 using the double-ring infiltrometer test (NF X 30-418, 2012). It's a classic method that is
185 widely used (Sidiras and Roth, 1987; Arriaga et al., 2010; Fatehnia et al., 2016). Thus, 30
186 measurements were carried out. It should be noted that, as shown in Fig. 4a, the soil surface
187 constituting the first centimetres (from 5 to 10 cm depth) of the wadi bed is completely
188 cracked. That is why during field measurements, and to prevent preferential flow paths, the
189 part of the cracked soil is completely cleared. Thus, the soil surface hydraulic conductivity
190 was measured at a depth between 5 and 10 cm. It is assumed that, at these depths, the
191 hydraulic conductivity measured is that of the older deposits induced by the dam's release
192 and/or rainfall. There were 30 other measurements that were made in the same positions, by
193 digging holes around 100 cm in depth, in order to evaluate the water infiltration in the
194 subsurface without surface deposits. As shown in Fig. 4b, even at depths beyond 50 cm,
195 cracks persist. In addition, 30 turbid water samples were taken from the retained water in
196 percolation tanks S1 and S3 for measuring their suspended solids concentrations.

197 **Fig.4**

198

199

200 **1.4. Laboratory investigations**

201 Laboratory analyses were performed on samples collected in the field. Among the
202 analyses carried out were

203 *i)* measurement of the saturated hydraulic conductivity of the layers formed on soil surface
204 (cake) using a triaxial permeameter according to ASTM D5084-10 (2010);

205 *ii)* percentage of organic matter (OM) in the cake. To evaluate this, the loss-on-ignition (LOI)
206 method was used. The LOI method consists of a known soil mass being placed in a ceramic
207 crucible ($\leq 10\text{g}$), which is then heated at 440°C overnight (ASTM D2974-14, 2014). Then they
208 are cooled in a desiccator and weighed. The OM content is determined as the difference
209 between the initial mass and the final mass of the sample divided by the initial mass of the
210 sample multiplied by 100%. A dozen of samples were tested;

211 *iii)* particle size distribution (PSD) of the deposited particles in the surface and subsurface
212 (columns depth); the PSD is measured using laser granulometer (Mastersizer, 2000);

213 *iv)* Atterberg limits. The liquid limit w_L and plastic limit w_P of the soil covering the surface of
214 the recharge sites, before and after the studied period, were measured according to NF EN
215 ISO 17892-12 (E), 2018 and *v)* mineralogical characterisation of the deposited particles using

216 X-ray diffraction (XRD). XRD was performed on a PANalytical X'Pert powder
217 diffractometer equipped with a $\text{CoK}\alpha$ anode ($\lambda = 1.7903 \text{ \AA}$) powered at 40 kV and 40 mA.

218 The detector was a linear PIXcel 1D detector equipped with 0.04 rad Soller slits. A powder
219 scan was performed on a sample that was back-loaded in a specific sample holder.

220 Programmable anti-scatter slits had a fixed aperture of $1/2^\circ$, whereas the anti-diffusion slits
221 had an aperture of 1° . A 15 mm mask was selected. The scans were performed in the $5\text{--}100^\circ$

222 range in steps of 0.0131° (399 s/step). The samples were also continually rotated at 8 sec/turn
223 in order to minimise preferred orientation. In order to characterise the clay fraction, oriented

224 mounts were also prepared from the supernatant of a clay/ultrapure water fraction. The
 225 supernatant was dropped on microscope glass slides and allowed to dry. These mounts were
 226 then measured by XRD as prepared, after exposure to ethylene glycol or after heating to
 227 550°C for 5 h in a furnace. Measurements were performed in duplicates. The weight fractions
 228 were estimated using the Relative Intensity Ratio (RIR) method implemented in software
 229 PANalytical high score (v.3.0.5).

230

231 **Hydraulic conductivity estimation**

232 To display the clogging of the sand filled columns, the saturated hydraulic
 233 conductivity drop as a consequence of the particles deposition is estimated on the basis of the
 234 Kozeny-Carman equation as follows:

$$235 \quad \frac{k}{k_0} = \frac{\phi^3}{\phi_0^3} \frac{(1-\phi_0)^2}{(1-\phi)^2} \frac{S_0^2}{S^2} \left(\frac{T_0}{T}\right)^2 \quad (1)$$

236 k_0 and k are the initial and reduced hydraulic conductivity values, respectively. S_0 and S are
 237 the specific surface area of the clean sand and the clogged sand, respectively. T_0 and T are,
 238 respectively, the tortuosity of the clean and clogged sand.

239 The specific surface area S of the clogged sand is estimated as follows (Alem et al., 2013):

$$240 \quad S = \frac{1}{1-\phi} \left[(1-\phi_0)S_0 + (1-\phi_d) \frac{\sigma}{\rho_p} S_p \right] \quad (2)$$

241 ϕ_d , ρ_p and S_p are the porosity, the particles specific density and the specific surface area of the
 242 deposited particles. σ is the retention defined as the volume of deposited particles per unit of
 243 porous-medium volume. The deposit porosity ϕ_d is derived from the average density of
 244 deposited particles as follows (Boller and Kavanaugh, 1995):

$$245 \quad \phi_d = 1 - \frac{\rho_d}{\rho_p} = 1 - \left[\frac{\rho_w}{\rho_p} + \left(1 - \frac{\rho_w}{\rho_p}\right) \frac{1}{a} N^{1-b} \right] \quad (3)$$

246 ρ_d is the average deposit density, ρ_w is the fluid density, N is the number of particles in a
 247 deposit layer and a and b are constants, taken as equal to 1 and 1.3, respectively.

248 Tortuosity is related to porosity as follows (De Marsily, 1986):

$$249 \quad T = F\phi \quad (4)$$

250 where $F = \phi^{-m}$ is the formation factor (Archie, 1942) given empirically as a function of
251 porosity, with $m=1.3$ for a sandy medium.

252

253 **2. Results and Discussion**

254 **2.1. Assessment of columns clogging**

255 **2.1.1. Subsurface clogging**

256 At the end of the study period (91 days), the implanted columns were recovered
257 (January 19, 2019). The results observed accumulation of fine particles in all columns filled
258 sand. As mentioned above (Section 1.3), each column was divided into 1 cm layers in order to
259 determine the mass of the particles deposited as a function of depth. Clogging that occurred in
260 columns could be divided into two types: superficial and internal clogging. The superficial
261 (surface) deposit (cake) on each column is discussed below in section 2.1.2.

262 Fig. 5a shows the particles deposition profiles in three columns (C_1 , C_2 and C_5)
263 implanted in recharge site S1. For clarity, only three profiles are represented for this site (S1).
264 Profiles illustrate that the amount of infiltrated particles is important in the column inlet and
265 decreases with depth. It means that suspended particles were trapped largely in the near-
266 surface layer that corresponds to the first 3 cm thick (internal clogging). In the study
267 presented by Page et al. (2014), a similar result was obtained. They showed that clogging was
268 concentrated in the top 3 cm of the columns.

269 Table 1 summarises the masses of the deposited particles in the first 3 centimetres and
270 those in the rest of the columns (from 3 to 30 cm). The average masses of the retained
271 particles in the first 3 cm thick layer of the columns implanted in sites S1, S2 and S3 equal 21
272 g, 15 g and 9g, respectively. Beyond 3 cm depth, the amount of retained particles (by sand)

273 ranges between 0 to 3 g/cm (Fig. 5a). It can be seen that the deposits in the first 3 centimetres
274 can reach over 30% of the total deposit measured in the columns.

275 **Table 1**

276 The damage to the porous medium, after 91 days of exposure to hydro-meteorological
277 conditions, as a result of particle deposition, was assessed by observing declines in either the
278 porosity or the hydraulic conductivity. Knowing the mass of the deposited particles in each
279 layer, the current porosity ϕ of the porous medium (sand + deposited particles) was estimated.
280 Porosity variation of the porous medium as a consequence of the particles deposition is
281 depicted in Fig. 5b, c and d. ϕ_0 is the initial porosity of the clean sand ($\phi_0=0.38$). The results
282 show that the porosity declines, on average, by 10 to 30% in the first 3 centimetres from the
283 top of the sand filled columns. Beyond this depth, the decrease in porosity varies between 2
284 and 8%.

285 **Fig.5**

286 **Fig.6**

287 The results plotted in Fig. 6 show variation of (k/k_0) predicted by equation (1) as a
288 function of the columns depth. For clarity, only three profiles are presented. Fig. 6 shows
289 clearly that the damage is not uniform in the sand-filled columns. Damage is important at the
290 inlet to the column and decreases with depth. In the first centimetres of the sand-filled
291 columns, k/k_0 reduced drastically, which is owed to the high amount of deposited particles in
292 the entrance of the columns and clogged up pores. This reduction can exceed 95% in the
293 immediate entrance of the columns. Beyond the first 10 centimetres, hydraulic conductivity
294 reduction varies between 10 and 40%. The same order of magnitude of hydraulic conductivity
295 reduction has been observed by Pavelic et al. (2011). They showed that physical clogging was
296 more significant than other forms of clogging and that the relative hydraulic conductivity
297 (k/k_0) declined to around 90% in some columns.

298 **2.1.2. Surface clogging**

299 Surface clogging (or external clogging) occurs when the suspended particles with size
300 larger than the pore diameters are intercepted in the surface. On the surface of the columns
301 implanted in the wadi bed, a layer due the particles deposition was developed. The
302 measurement of the solid particles concentration was done in the Percolation tanks (S1 and
303 S3) for the turbid water before it cross the embankment were ranged from 1.1 to 1.4 g/L.

304 The thickness and the mass of the deposited particles (cake) on surface of each column
305 are presented in Table 2. The thickness of the cake formed above each column filled with
306 sand ranged from 0 to 7 cm. Indeed, an average cake thickness of 2.2 cm can be retained.
307 Notice that when the thicknesses of the formed cake were measured, their average water
308 content was about 29%. The results show that the cake thickness depends on the position of
309 the implanted columns. Thus, columns C₁, C₆, C₇ and C₁₀, implanted near the embankments
310 facilities, receive a high deposit volume, caused by embankments-break flows charged by
311 suspended particles.

312 **Table 2**

313 This important deposit generates a total clogging of the implanted columns. As shown
314 above (section 2.1.1), the deposition in the first 3 centimetres of the sand-filled columns
315 drastically reduces its hydraulic conductivity (a drop more than 50%, on average, was
316 measured). Thus, one can assume that the cake completely controls the hydraulic conductivity
317 of the sand, which can be considered as totally clogged.

318

319 **2.1.3. Characterisation of the cake's particles**

320 In this section, the percentage of organic matter (OM) and the mineralogical
321 characterisation of the particles constituting the cake formed on the surface are presented.

322 Results indicate an average percentage of OM around 3%. Thus, it can be considered that the
323 amount of total organic carbon in the total mass analysed is low.

324 Analysis of cake particles by X-ray diffraction (XRD) was used to achieve two main
325 objectives: i) obtaining a general idea of the mineralogical composition of the particles
326 constituting the cake and ii) evaluating the presence of certain clay minerals, which are highly
327 reactive in the presence of water, such as smectite and montmorillonite. Their clogging
328 potential is prejudicial for water infiltration (Mays and Hunt, 2007).

329 The results are shown in Fig. 7. The sample contained several minerals including
330 quartz (50%), calcite (20%) and dolomite (10%). The remaining sample fraction was
331 attributed to the presence of various clays, namely vermiculite, an interstratified illite-
332 vermiculite and two kaolinite polytypes (halloysite 7Å and dickite). The halloysite:dickite
333 ratio was estimated using the RIR method at 15:2. It is noted that the results show the absence
334 of smectite and montmorillonite, two clay minerals that swell quickly in the presence of
335 water, leading to a rapid clogging of the pores.

336 **Fig.7**

337

338 **2.1.4. Particles size distribution of the deposited particles**

339 Fig. 8 shows the PSD of the retained particles in the surface (cake) and subsurface of
340 the columns. The distribution of the retained particles in the columns' subsurface were
341 measured every 5 cm of depth (0–5 cm; 5–10 cm; 10–15 cm; 15–20 cm; 20–25cm and 25–30
342 cm). For clarity, only three PSD are presented in Fig. 8.

343 The PSD of the retained particles in columns show a very slight differences in the
344 particle size distribution as a function of the depth. However, there is a slight tendency
345 towards decreasing the size of the particles retained with the depth. 90% of particles that

346 infiltrated the sand-filled columns were less than 25 μm . An average median diameter around
347 6 μm was measured (Table 3).

348 The PSD of the particles constituting the cake (surface deposits) indicate a wider
349 distribution up to 600 μm . The PSD presented in Fig. 8 is representative of all that measured
350 for the different analysed samples. The average median diameter measured for the particles
351 retained in surface was 25 μm . Also, as indicated in Table 3, more than 34% of the particles
352 constituting the cake are greater than 63 μm . More than 50% of the particles deposited on
353 MAR surface ranged between 30 and 400 μm . These results confirm what was expected, i.e.
354 the largest particles are mainly retained at the columns' surfaces.

355 In this study, among the mechanism involved in the retention of the suspended
356 particles in the subsurface, straining dominates; however, on the surface, straining and
357 sedimentation are the two mechanisms that affect particle retention.

358 Straining of the particles in porous media depends on the ratio of d_{p50}/d_{g50} , where d_{p50}
359 is the median diameter of the suspended particles and d_{g50} is the median diameter of the grains
360 constituting the porous medium. As reported by Bradford et al. (2003), straining occurs when
361 the d_{p50}/d_{g50} ratio is greater than approximately 0.005. The median grain diameter of the used
362 sand in this study was $d_{g50} = 520 \mu\text{m}$, and the median diameter of suspended particles
363 infiltrated in the sand filled columns was $d_{p50} = 6 \mu\text{m}$ (Table 3). The ratio of d_{p50}/d_{g50} equals
364 0.011, which leads to significant particles retention by straining in sand.

365 As discussed above, for surface deposition, larger particles were retained, and then the
366 ratio of d_{p50}/d_{g50} equalled 0.048. Retention of larger particles by straining in the surface of the
367 sand has actively participated in the filtration of particles of all sizes, including the finest, thus
368 preventing their transport in deep, favouring surface clogging.

369 These results clearly show the extent of the low rainfall (during 91 days) to promote
370 the mobilisation and transport of suspended particles carried by runoffs. They reveal that

371 despite the high grain size distribution of the sand used, unlike the natural soil of the recharge
372 sites, there is a significant clogging on the surface.

373

374 **Fig.8**

375 **Table 3**

376

377 **2.2. Assessment of sites clogging**

378 **2.2.1. Distribution of surface clogging on the studied sites**

379 To quantify the thickness of the deposited particles on natural soil of the wadi bed,
380 many pickets were placed at different positions of the recharge sites over a large area (~750
381 m²). As shown in Fig. 9, deposits accumulation varied significantly according to the distance
382 to the embankment. Investigations undertaken over 91 days indicate that, even with the low
383 rainfall, the thickness of the accumulated deposits is important and ranges between 0 and 12
384 cm, with an average of 2.5 cm. For site S1, the accumulated deposit reaches thicknesses
385 greater than 2 cm, at a distance of 40 metres from the embankment. However, this thickness is
386 reached in site S3 at a distance of 20 m from the embankment. This observation can be
387 justified by the position of the recharge sites; thus, site S1, which is upstream of sites S2 and
388 S3, retains more particles transported by the flows. Also, many factors can affect the cake
389 thickness such as wadi bed topography, presence of surface preferential flow and vegetation
390 density. In some picket positions, the cake thickness reached up to 6 cm (Fig. 9b), which is
391 owed to topographical depressions (bowl-shaped) where a significant volume of water
392 stagnates and favours more particles deposition. In contrast, suspended particles deposition
393 was distributed fairly evenly throughout site S1 (Fig. 9a), except on the right bank where
394 more deposits were observed. Among possible interpretation of the latter observation, the lack
395 of vegetation on the right bank favoured surface erosion from the bank during rainfall. As a

396 consequence, high accumulations were observed compared to the left bank which is covered
397 with vegetation.

398 Note that it has been observed that some large cracks (aperture of 3 or 4 cm) do not
399 close completely even if after several days of rain accompanying high water level (20 to 30
400 cm) in the recharge site. However, their depth has decreased, which is owed to the suspended
401 particles deposition.

402 **Fig. 9**

403 **2.2.2 Hydraulic conductivity**

404 In this part, we discuss the hydraulic conductivity of the soil that controls the water
405 infiltration from the recharge sites surface to the subsurface soil and therefore to the aquifer.
406 For this purpose, as discussed above, *in situ* saturated hydraulic conductivity measurements at
407 the surface and subsurface (around 100 cm depth) have been carried out using the double
408 rings infiltrometer (Cf. section 1.3).

409 For all sites and for surface and subsurface measurements, saturated hydraulic
410 conductivity varies from 8.33×10^{-5} to 1.67×10^{-6} , with an average value of 4.25×10^{-5} m/s. For
411 example, in site S3, an average value of 3×10^{-5} ($\pm 2 \times 10^{-6}$) m/s and 6×10^{-5} ($\pm 3 \times 10^{-6}$) were
412 obtained for k measurements in the surface and subsurface, respectively. These measured k
413 values are low for silty-clayey soil but can be explained by the presence of micro cracks. As
414 discussed above (section 1.3), cracks exist in the surface and the subsurface (Fig. 4) of the
415 tested soils, and their presence increases water infiltration rate.

416 The measurement of the hydraulic conductivity of the cake represents a main element
417 for assessing clogging. To evaluate the hydraulic conductivity of the formed cake without
418 cracks, measurements were made on cake samples taken after the 91 days investigation, either
419 on the columns surfaces or around the pickets. Hydraulic conductivity of the cake was
420 determined by using a triaxial permeameter system. An example of measurements of the

421 hydraulic conductivity of the cake, under different confining pressure ranging from the
422 greatest pressure (300 kPa) to the smallest (20 kPa), is presented in Fig. 10. The hydraulic
423 conductivity of the cake under zero confining pressure is obtained by extrapolation of the
424 curve (Fig. 10), and an average value of 4×10^{-8} m/s was retained.

425 **Fig.10**

426 Clayey soils tend to crack when drying (Morris et al., 1992). The resulting cracking
427 causes crucial problems in geo-environmental engineering and dramatically affects hydraulic
428 conductivity (Peron et al., 2009). Silty-clayey soil of El Himmer wadi bed has been submitted
429 to several wetting and drying (W-D) cycles due to seasonal variations, including temperatures
430 and rainfall. As a result of soil desiccation, cracks are created at the surface and in depth (Cf.
431 Fig. 4). As mentioned above, the measured hydraulic conductivity in laboratory by triaxial
432 permeameter is in the range of 10^{-8} m/s. However, measurements undertaken in the field using
433 the double rings infiltrometer revealed a hydraulic conductivity that varies between 10^{-5} and
434 10^{-6} m/s. The ratio between the hydraulic conductivity measured in field and that obtained in
435 laboratory (k_{field}/k_{lab}) can reach 10^3 . Despite the difference between the two techniques of
436 measurement and the difference in observation scale, the difference between the measured
437 values in laboratory and in the field remains significant. It is very low for non-cracked
438 samples and very high for cracked soils. Based on the experimental studies in laboratory,
439 several studies have been conducted on the effect of a cracks network on hydraulic
440 conductivity in clayey soil. Louati et al. (2018) showed that after three W-D cycles and for all
441 tested samples with different initial densities, the hydraulic conductivity increased in the
442 presence of cracks. Lu et al. (2015) also concluded that after a four W-D cycles; the
443 conductivity increased from 8.3×10^{-9} to 1.5×10^{-7} m/s for compacted clay.

444 However, as reported by Rayhani et al. (2008), during the periods of rainfall (wetting
445 cycles) that follow periods of evaporation (drying cycles), water fills cracked soil. The

446 hydrostatic forces increased, and the water is slowly absorbed by the clay. The effect of the
447 absorption is to increase the unit weight of the clay as well as to reduce the unit weight of its
448 shear strength. As a result of these processes, the driving forces (sliding) increase at the same
449 time as the resistance forces (shear strength) decrease. During water filling, cracks tend to
450 disappear and hydraulic conductivity decreases. This process can be carried out rapidly in
451 clayey soil with high plasticity index (Rayhani et al., 2008). This phenomenon is known as
452 the "self-healing".

453 In this study, before and after the studied period, the liquid limit w_L and plastic limit
454 w_P of the soil covering the surface of the recharge sites were measured. The obtained results
455 indicate that $w_L = 66\%$ and $w_P = 32\%$. Thus, the plasticity index I_p equals 34%.

456 After water infiltration in the studied sites, a slight reduction of the cracks opening in
457 some locations was observed, which can be attributed to the self-healing due to the high
458 plasticity index of the silty-clayey soil. In other locations, the cracks were filled entirely or
459 partially by the particles transported by flows. Indeed, in the periods of high precipitations
460 and, therefore, with a large contribution to the suspended particles deposition (sediment
461 supply) in the recharge sites, deposits that form the cake could reduce the saturated hydraulic
462 conductivity by 1,000 orders of magnitude in comparison to those measured during dry
463 period. Thus, the hydraulic conductivity reduction generates less infiltration towards the
464 subsurface, which is owed to evaporation.

465

466 **3. Recommendations for monitoring clogging sites**

467 Various factors can reduce infiltration rates in recharge sites. Physical clogging,
468 predominantly related to a filter cake forming, is usually the most important factor.
469 Management approaches were developed to reduce clogging effects and renovate recharge
470 rates. To manage site clogging, recommendations exist such as deposits removal and scraping

471 (Mousavi and Rezai, 1999; Gale and Dillon, 2005), use of gravel filters (Hatt et al., 2007) and
472 vegetation cultivation (Woo et al., 1997; Gonzalez-Merchan et al., 2014; Al-Maktoumi et al.,
473 2017).

474 To extend bed life of recharge sites in wadi El Himmer, there are three
475 recommendations: i) a regular scraping of clogged layers. Due to the cake thickness measured
476 in this study, it is thought that at least one scraping per year is necessary for a depth of 10 to
477 20 cm. The scraping technique must be recurrent as long as these sites are exploitable. ii) The
478 second recommendation, with lasting effects, is planting shrubs in the upstream of MAR sites
479 and on the wadi banks, which could reduce fine particles transport and their deposition in
480 MAR sites. Also, as discussed above, as infiltration is controlled by cracks (Römken and
481 Prasad, 2006; Dunkerley, 2008; Greve et al., 2010), the reduction of particles contribution
482 towards these sites will make it possible to exploit the presence of these cracks systems to
483 maximise recharge. This last technique (vegetation) would reduce the number of scraping
484 intervention on the sites. Thus, it is thought that the cultivation of the *Stipa tenacissima*
485 upstream of the MAR sites can be a good solution. As reported by Eldridge et al. (2010), the
486 shrub *Stipa tenacissima* can enhance the sorptivity and infiltration 2–3 times higher than in
487 intact on soil crusts. In addition, this shrub is adapted to the silty soil and to arid and semi-arid
488 climates (Ghiloufi et al., 2015), which makes it suitable for cultivation in an environment
489 characterised by increasing degradation of water resources (Ramírez et al., 2007). Cultivation
490 of the shrub *Stipa tenacissima* in wadi El Himmer represents a hydro-ecological solution; it is
491 clean, less expensive and more efficient for limiting particles transfer and renovating
492 infiltration through the wadi bed. iii) The third recommendation consists of the construction
493 of a settling basin upstream of the recharge sites, supplied by rainwater during floods and dam
494 releases; this may be useful for reducing flow rates and the sedimentation rate of downstream
495 recharge sites.

496 Therefore, an experimental model should be developed even before the construction of
497 the recharge facilities, in order to predict or estimate the impact of clogging in MAR sites.
498 Moreover, the data generated by the model can be easily integrated into the cost–benefit ratio
499 of the models, making it possible to predict the most cost-effective cleaning strategies (Phipps
500 et al., 2006), in order to improve the percolation efficiency of the MAR and minimise the
501 operating costs.

502 **Conclusions**

503 This study was undertaken to investigate the extent of clogging in Managed Aquifer
504 Recharge (MAR) sites in wadi El Himmer (Berrechid, Morocco) over 91 days. To evaluate
505 the *in situ* clogging, sand-filled columns and pickets were implanted in the wadi bed. Results
506 indicate that, although the low rainfall during the studied period, clogging that occurred in
507 wadi bed is significant. The thickness of the deposited particles forming a cake (surface
508 clogging) is important and drastically reduces the hydraulic conductivity of the wadi bed soil.
509 A 1,000 order of magnitude can be reached during the wetting cycles when the cake formed is
510 cracks free. The obtained results from the columns show damage to the sand medium that is
511 owed to surface and subsurface clogging. The main mechanism involved in the sand clogging,
512 either in the surface or subsurface, is straining. Because of the large particle size distribution
513 of the particles carried by the flow, more than 50% of the particles deposited on MAR surface
514 ranged between 30 and 400 μm . Hydraulic conductivities measured *in situ* during the drying
515 period are in the order of 10^{-5} m/s and are affected by the presence of cracks that promote
516 infiltration. However, due to the high plasticity index of the MAR soil, a slight reduction of
517 the cracks opening during wetting cycles is observed. In addition, contribution of fine
518 particles deposited in these cracks would participate actively in the reduction of hydraulic
519 conductivity.

520 Despite the low rainfall (an average of 1.34 mm/day) and the short period (91 days) of
521 this investigation, MAR sites clogging is effective; the thickness of the deposits exceeds 3 cm
522 in a large part of the MAR. However, a long-term study is necessary to more precisely
523 evaluate the role of cracks under cyclic drying and wetting.
524

Acknowledgements

This study is supported by PHC TOUBKAL project (18/74): Campus France N° 38951NJ.
The authors wish to thank the Bouregreg and Chaouia Hydraulic Basin Agency (ABHBC)
for the providing the climate data.

References

- 525
526 Alem, A., Elkawafi, A., Ahfir, N.-D., Wang, H., 2013. Filtration of kaolinite particles in a saturated
527 porous medium: hydrodynamic effects. *Hydrogeol. J.* 3, 573–586.
528 <https://doi.org/10.1007/s10040-012-0948-x>
- 529 Al-Maktoumi A., Kacimov A., Suzanne F., Al-Busaidi H., Al-Ismaily S., Al-Mayahi A., Al-
530 Khanbashi S., 2017. Experimental study of clogging of subsurface pores in the vicinity of
531 dams in arid zones: groundwater recharge efficiency and potential solution. 9th International
532 Conference on Porous Media & Annual Meeting, Rotterdam, 8-11 May, 2017
- 533 Archie, G.E., 1942. The Electrical Resistivity Log as an Aid in Determining Some Reservoir
534 Characteristics. *Trans. AIME* 146, 54–62. <https://doi.org/10.2118/942054-G>
- 535 Arriaga, F.J., Kornecki, T.S., Balkcom, K.S., Raper, R.L., 2010. A method for automating data
536 collection from a double-ring infiltrometer under falling head conditions. *Soil Use Manag.* 26,
537 61–67. <https://doi.org/10.1111/j.1475-2743.2009.00249.x>
- 538 ASTM D2974-14, 2014. Standard test methods for moisture, ash, and organic matter of peat and other
539 organic soils. ASTM International, West Conshohocken, PA.
- 540 ASTM D5084-10, 2010. Standard test methods for measurement of hydraulic conductivity of saturated
541 porous materials using a Flexible wall permeameter, ASTM International, West
542 Conshohocken, PA

543 Blaschke, A.P., Steiner, K.H., Schmalfluss, R., Gutknecht, D., Sengschmitt, D., 2003. Clogging
544 processes in hyporheic interstices of an impounded river, the Danube at Vienna, Austria. *Int.*
545 *Rev. Hydrobiol.* 88 (3–4), 397–413. <https://doi.org/10.1002/iroh.200390034>

546 Boller, M.A., Kavanaugh, M.C., 1995. Particle characteristics and headloss increase in granular media
547 filtration. *Water Res.* 29, 1139–1149. [https://doi.org/10.1016/0043-1354\(94\)00256-7](https://doi.org/10.1016/0043-1354(94)00256-7)

548 Bouwer, H., 2002. Artificial recharge of groundwater: hydrogeology and engineering. *Hydrogeol. J.*
549 10, 121–142. <https://doi.org/10.1007/s10040-001-0182-4>

550 Bradford, S.A., Simunek, J., Bettahar, M., van Genuchten, M.Th., Yates, S.R., 2003. Modeling
551 Colloid Attachment, Straining, and Exclusion in Saturated Porous Media. *Environ. Sci.*
552 *Technol.* 37, 2242–2250. <https://doi.org/10.1021/es025899u>

553 Casas-Mulet, R., Alfredsen, K.T., McCluskey, A.H., Stewardson, M.J., 2017. Key hydraulic drivers
554 and patterns of fine sediment accumulation in gravel streambeds: A conceptual framework
555 illustrated with a case study from the Kiewa River, Australia. *Geomorphology* 299, 152–164.
556 <https://doi.org/10.1016/j.geomorph.2017.08.032>

557 De Marsily, G., 1986. *Quantitative Hydrogeology: Groundwater Hydrology for Engineers*. Academic,
558 New York

559 Detay, M., 1995. *Rational Ground Water Reservoir Management: The Role of Artificial Recharge*.
560 Presented at the Artificial Recharge of Ground Water II, ASCE, pp. 231–240.

561 Dillon, P.J., Vanderzalm, J., Page, D., Barry, K., Gonzalez, D., Muthukaruppan, M., Hudson, M.,
562 2016. Analysis of ASR Clogging Investigations at Three Australian ASR Sites in a Bayesian
563 Context. *Water* 8(10), 442. <https://doi.org/10.3390/w8100442>

564 Dillon, P., Pavelic, P., Page, D., Beringen, H., Ward, J., 2009. Managed aquifer recharge: An
565 Introduction. *Waterlines Report Series No. 13*. <https://doi.org/10.1007/s10040-004-0413-6>

566 Dillon, P.J., 2005. Future management of aquifer recharge. *Hydrogeol. J.* 13 (1), 313–316
567 <https://doi.org/10.1007/s10040-004-0413-6>

568 Pavelic, P., & Dillon, P. J. (1997). Review of international experience in injecting natural and
569 reclaimed waters into aquifers for storage and reuse. *Centre for Groundwater Studies Rep.*
570 No. 74

571 Dunkerley, D.L., 2008. Bank permeability in an Australian ephemeral dry-land stream: variation with
572 stage resulting from mud deposition and sediment clogging. *Earth Surf. Proc. Land.* 33 (2),
573 226–243. <https://doi.org/10.1002/esp.1539>

574 El Assaoui, N., Amraoui, F., El Mansouri, B., 2015. Modeling of Climate Changes Impact on
575 Groundwater Resources of Berrechid Aquifer 4, 15. *Int. j. innov. res. sci. eng. technol.* [https://](https://doi.org/10.15680/IJIRSET.2015.0407118)
576 DOI:10.15680/IJIRSET.2015.0407118

577 Eldridge, D.J., Bowker, M.A., Maestre, F.T., Alonso, P., Mau, R.L., Papadopoulos, J., Escudero, A.,
578 2010. Interactive effects of three ecosystem engineers on infiltration in a semi-arid

579 Mediterranean grassland. *Ecosystems* 13, 499–510. [https://doi.org/10.1007/s10021-010-9335-](https://doi.org/10.1007/s10021-010-9335-4)
580 4

581 El Ghali, T., Marah, H., Qurtobi, M., Raibi, F., Bellarbi, M., Amenzou, N., El Mansouri, B., 2020.
582 Geochemical and isotopic characterization of groundwater and identification of
583 hydrogeochemical processes in the Berrechid aquifer of central Morocco. *Carbonates and*
584 *Evaporites*, 35(2), 1-21. <https://doi.org/10.1007/s13146-020-00571-y>

585 El Mansouri, B., 1993. Structure et modélisation quantitative de l'aquifère de Berrechid (Maroc) :
586 Validation par l'approche géostatistique (thesis). Lille 1.

587 Famiglietti, J.S., 2014. The global groundwater crisis. *Nat. Clim. Change* 4, 945–948.
588 <https://doi.org/10.1038/nclimate2425>

589 Fatehnia, M., Paran, S., Kish, S., Tawfiq, K., 2016. Automating double ring infiltrometer with an
590 Arduino microcontroller. *Geoderma* 262, 133–139.
591 <https://doi.org/10.1016/j.geoderma.2015.08.022>

592 Fetzer, J., Holzner, M., Plötze, M., Furrer, G., 2017. Clogging of an Alpine streambed by silt-sized
593 particles – Insights from laboratory and field experiments. *Water Res.* 126, 60–69.
594 <https://doi.org/10.1016/j.watres.2017.09.015>

595 Gale, I., Dillon, P., 2005. Strategies for Managed Aquifer Recharge (MAR) in Semiarid Areas.
596 UNESCO-IHP, Paris

597 Gaskin, S.J., Pieterse, J., Shafie, A.A., Lepage, S., 2003. Erosion of undisturbed clay samples from the
598 banks of the St. Lawrence River. *Can. J. Civ. Eng.* 30, 585–595. [https://doi.org/10.1139/103-](https://doi.org/10.1139/103-008)
599 008

600 Ghiloufi, W., Quero Pérez, J.L., García-Gómez, M., Chaieb, M., 2015. Assessment of species
601 diversity and state of *Stipa tenacissima* steppes. *Turk. J. Bot.* 39, 227–237.
602 <https://doi.org/10.3906/bot-1404-57>

603 Gonzalez-Merchan, C., Barraud, S., Bedell, J.-P., 2014. Influence of spontaneous vegetation in
604 stormwater infiltration system clogging. *Environ. Sci. Pollut. Res.* 21, 5419–5426.
605 <https://doi.org/10.1007/s11356-013-2398-y>

606 Gonzalez-Merchan, C., Barraud, S., Coustumer, S.L., Fletcher, T., 2012. Monitoring of clogging
607 evolution in the stormwater infiltration system and determinant factors. *Eur. J. Environ. Civ.*
608 *Eng.* 16, s34–s47. <https://doi.org/10.1080/19648189.2012.682457>

609 Greve, A., Andersen, M., Acworth, M., 2010. Investigations of soil cracking and preferential flow in a
610 weighing lysimeter filled with cracking clay soil. *J. Hydrol.* 393, 105–113.
611 <http://dx.doi.org/10.1016/j.jhydrol.2010.03.007>

612 Hatch, C.E., Fisher, A.T., Ruehl, C.R., Stemler, G., 2010. Spatial and temporal variations in streambed
613 hydraulic conductivity quantified with time-series thermal methods. *J. Hydrol.* 389 (3–4),
614 276–288. <https://doi.org/10.1016/j.jhydrol.2010.05.046>

615 Hatt, B.E., Fletcher, T.D., Deletic, A., 2007. Treatment performance of gravel filter media:
616 implications for design and application of stormwater infiltration systems. *Water Res.*
617 41:2513–2524. <https://doi.org/10.1016/j.watres.2007.03.014>

618 Hazan, R.M., Moullard, L., 1962. Notice hydrogéologique de la plaine de Berrechid. Rabat.

619 Houston, S.L., Duryea, P.D., Hong, R., 1999. Infiltration Considerations for Ground-Water Recharge
620 with Waste Effluent. *J. Irrig. Drain. Eng.* 125, 264–272. [https://doi.org/10.1061/\(ASCE\)0733-](https://doi.org/10.1061/(ASCE)0733-9437(1999)125:5(264))
621 9437(1999)125:5(264)

622 Hutchison, A., Milczarek, M., Banerjee, M., 2013. Clogging Phenomena Related to Surface Water
623 Recharge Facilities, in: *Clogging Issues Associated with Managed Aquifer Recharge Methods.*
624 Australia, p. 25.

625 Jeong, H.Y., Jun, S.-C., Cheon, J.-Y., Park, M., 2018. A review on clogging mechanisms and
626 managements in aquifer storage and recovery (ASR) applications. *Geosci. J.* 22, 667–679.
627 <https://doi.org/10.1007/s12303-017-0073-x>

628 Louati, F., Trabelsi, H., Jamei, M., Taibi, S., 2018. Impact of wetting-drying cycles and cracks on the
629 permeability of compacted clayey soil. *Eur. J. Environ. Civ. Eng.* 0, 1–26.
630 <https://doi.org/10.1080/19648189.2018.1541144>

631 Lu, H., Liu, J., Li, Y., Dong, Y., 2015. Heat Transport and Water Permeability during Cracking of the
632 Landfill Compacted Clay Cover. *J. Chem.* vol. 2015. <https://doi.org/10.1155/2015/685871>

633 Marino, M.A., 1975. Artificial groundwater recharge, I. Circular recharging area. *J. Hydrol.* 25, 201–
634 208. [https://doi.org/10.1016/0022-1694\(75\)90021-9](https://doi.org/10.1016/0022-1694(75)90021-9)

635 Mays, D.C., Hunt, J.R., 2007. Hydrodynamic and Chemical Factors in Clogging by Montmorillonite
636 in Porous Media. *Environ. Sci. Technol.* 41, 5666–5671. <https://doi.org/10.1021/es062009s>

637 Missimer, T. M., Guo, W., Maliva, R. G., Rosas, J., Jadoon, K. Z., 2015. Enhancement of wadi
638 recharge using dams coupled with aquifer storage and recovery wells. *Environ. Earth Sci.*
639 73(12), 7723–7731. <https://doi.org/10.1007/s12665-014-3410-7>

640 Morris, P.H., Graham, J., Williams, D.J., 1992. Cracking in drying soils. *Can. Geotech. J.* 29, 263–
641 277. <https://doi.org/10.1139/t92-030>

642 Mousavi, S.-F., Rezai, V., 1999. Evaluation of scraping treatments to restore initial infiltration
643 capacity of three artificial recharge projects in central Iran. *Hydrogeol. J.* 7 (5), 490–500.
644 <https://doi.org/10.1007/s100400050222>

645 NF EN ISO 17892-12 (E), 2018. Geotechnical investigation and testing - Laboratory testing of soil -
646 Part 12: Determination of liquid and plastic limits.

647 NF X 30-418, 2012. Determination of the vertical permeability coefficient of a land using the open-
648 type double-ring infiltrometer test.

649 Nie, J.Y., Zhu, N.W., Zhao, K., Wu, L., Hu, Y.H., 2011. Analysis of the bacterial community changes
650 in soil for septic tank effluent treatment in response to bio-clogging. *Water Sci. Technol.* 63,
651 1412–1417. <https://doi.org/10.2166/wst.2011.319>

652 Ouassissou, R., Kuper, M., Dugue, P., El Amrani, M., Ameer, F., 2019. Rivalités et arrangements
653 coopératifs pour l'accès à l'eau souterraine dans la plaine de Berrechid au Maroc. *Cah. Agric.*
654 <https://doi.org/10.1051/cagri/2019006>

655 Page, D., Vanderzalm, J., Miotliński, K., Barry, K., Dillon, P., Lawrie, K., Brodie, 32 R.S., 2014.
656 Determining treatment requirements for turbid river water to avoid clogging of aquifer storage
657 and recovery wells in siliceous alluvium. *Water Res.* 66, 99–110.
658 <https://doi.org/10.1016/j.watres.2014.08.018>

659 Pavelic, P., Dillon, P.J., Mucha, M., Nakai, T., Barry, K.E., Bestland, E., 2011. Laboratory assessment
660 of factors affecting soil clogging of soil aquifer treatment systems. *Water Res.* 45(10), 3153–
661 3163. <https://doi.org/10.1016/j.watres.2011.03.027>

662 Peron, H., Hueckel, T., Laloui, L., Hu, L.B., 2009. Fundamentals of desiccation cracking of fine-
663 grained soils: experimental characterisation and mechanisms identification. *Can. Geotech. J.*
664 46, 1177–1201. <https://doi.org/10.1139/T09-054>

665 Phipps, D., Lyon, S., Hutchinson, A. S., 2006. Development of a percolation decay model to guide
666 future optimization of surface water recharge basins. In *Management of Aquifer Recharge for*
667 *Sustainability, Proceedings of the 6th International Symposium on Managed Artificial*
668 *Recharge of Groundwater, ISMAR6, Phoenix, AZ, USA (Vol. 28). ISO 690*

669 Pholkern, K., Srisuk, K., Grischek, T., Soares, M., Schäfer, S., Archwchai, L., Saraphirom, P.,
670 Pavelic, P., Wirojanagud, W., 2015. Riverbed clogging experiments at potential river bank
671 filtration sites along the Ping River, Chiang Mai, Thailand. *Environ. Earth Sci.* 73, 7699.
672 <http://dx.doi.org/10.1007/s12665-015-4160-x>.

673 Ramírez, D.A., Bellot, J., Domingo, F., Blasco, A., 2007. Can water responses in *Stipa tenacissima* L.
674 during the summer season be promoted by non-rainfall water gains in soil? *Plant Soil* 291, 67–
675 79. <http://dx.doi.org/10.1007/s11104-006-9175-3>.

676 Rayhani, M.H.T., Yanful, E.K., Fakher, A., 2008. Physical modeling of desiccation cracking in plastic
677 soils. *Eng. Geol.* 97, 25–31. <https://doi.org/10.1016/j.enggeo.2007.11.003>

678 Rinck-Pfeiffer, S., Ragusa, S., Sztajn bok, P., Vandevelde, T., 2000. Interrelationships between
679 biological, chemical, and physical processes as an analog to clogging in aquifer storage and
680 recovery (ASR) wells. *Water Res.* 34, 2110–2118. [https://doi.org/10.1016/S0043-](https://doi.org/10.1016/S0043-1354(99)00356-5)
681 [1354\(99\)00356-5](https://doi.org/10.1016/S0043-1354(99)00356-5)

682 Römken, M., Prasad, S., 2006. Rain infiltration into swelling/shrinking/cracking soils. *Agric. Water*
683 *Manag.* 86 (1), 196–205. <https://doi.org/10.1016/j.agwat.2006.07.012>

684 Ruhard, j. P., 1975. Chaouia et la plaine de Berrechid (Tome 1), in: *Ressources En Eau Du Maroc*. p.
685 231.

686 Ryan, P.A., 1991. Environmental effects of sediment on New Zealand streams: A review. *New*
687 *Zealand journal of marine and freshwater research* 25, 207–221.
688 <https://doi.org/10.1080/00288330.1991.9516472>

689 Sadiki, M. L., El Mansouri, B., Benseddik, B., Chao, J., Kili, M., El Mezouary, L., 2019. Improvement
690 of groundwater resources potential by artificial recharge technique: A case study of Charf El
691 Akab aquifer in the Tangier region, Morocco. *J. Groundw. Sci. Eng. Journal of Groundwater
692 Science and Engineering* 7, 224–236. [https://doi.org/DOI: 10.19637/j.cnki.2305-](https://doi.org/DOI: 10.19637/j.cnki.2305-7068.2019.03.003)
693 7068.2019.03.003

694 Schubert, J., 2002. Hydraulic aspects of riverbank filtration—field studies. *J. Hydrol., Attenuation of
695 Groundwater Pollution by Bank Filtration* 266, 145–161 . [https://doi.org/10.1016/S0022-](https://doi.org/10.1016/S0022-1694(02)00159-2)
696 1694(02)00159-2

697 Sepaskhah, A.R., Sokoot, M., 2010. Effects of wastewater application on saturated hydraulic
698 conductivity of different soil textures. *J. Plant Nutr. Soil Sci.* 173, 510–516.
699 <https://doi.org/10.1002/jpln.200800220>

700 Sidiras, N., Roth, C.H., 1987. Infiltration measurements with double-ring infiltrometers and a rainfall
701 simulator under different surface conditions on an Oxisol. *Soil Tillage Res.* 9, 161–168.
702 [https://doi.org/10.1016/0167-1987\(87\)90082-1](https://doi.org/10.1016/0167-1987(87)90082-1)

703 Siegrist, R.L., 1987. Soil Clogging During Subsurface Wastewater Infiltration as Affected by Effluent
704 Composition and Loading Rate 1. *J. Environ. Qual.* 16, 181–187.
705 <https://doi.org/10.2134/jeq1987.00472425001600020016x>

706 Siriwardene, N.R., Deletic, A., Fletcher, T.D., 2007. Clogging of stormwater gravel infiltration
707 systems and filters: Insights from a laboratory study. *Water Res.* 41, 1433–1440.
708 <https://doi.org/10.1016/j.watres.2006.12.040>

709 Skolasińska, K., 2006. Clogging microstructures in the vadose zone—laboratory and field studies.
710 *Hydrogeol. J.* 14, 1005–1017. <https://doi.org/10.1007/s10040-006-0027-2>

711 Stefan, C., Ansems, N., 2018. Web-based global inventory of managed aquifer recharge applications.
712 *Sustain. Water Resour. Manag.* 4, 153–162. <https://doi.org/10.1007/s40899-017-0212-6>

713 Taylor, R.G., Scanlon, B., Döll, P., Rodell, M., van Beek, R., Wada, Y., Longuevergne, L., Leblanc,
714 M., Famiglietti, J.S., Edmunds, M., Konikow, L., Green, T.R., Chen, J., Taniguchi, M.,
715 Bierkens, M.F.P., MacDonald, A., Fan, Y., Maxwell, R.M., Yechieli, Y., Gurdak, J.J., Allen,
716 D., Shamsudduha, M., Hiscock, K., Yeh, P.J.F., Holman, I., Treidel, H., 2012. Ground water
717 and climate change. *Nat. Clim. Change.* [http:// dx.doi.org/10.1038/nclimate1744](http://dx.doi.org/10.1038/nclimate1744)

718 Treese, S., Meixner, T., Hogan, J.F., 2009. Clogging of an Effluent Dominated Semiarid River: A
719 Conceptual Model of Stream-Aquifer Interactions1. *JAWRA J. Am. Water Resour. Assoc.* 45,
720 1047–1062. <https://doi.org/10.1111/j.1752-1688.2009.00346.x>

721 Viviani, G., Iovino, M., 2004. Wastewater Reuse Effects on Soil Hydraulic Conductivity. *J. Irrig.
722 Drain. Eng.* 130, 476–484. [https://doi.org/10.1061/\(ASCE\)0733-9437\(2004\)130:6\(476\)](https://doi.org/10.1061/(ASCE)0733-9437(2004)130:6(476))

723 Woo, M.K., Fang, G., DiCenzo, P.D., 1997. The role of vegetation in the retardation of rill erosion.
724 *Catena* 29, 145–159. [https://doi.org/10.1016/S0341-8162\(96\)00052-5](https://doi.org/10.1016/S0341-8162(96)00052-5)

FIGURES

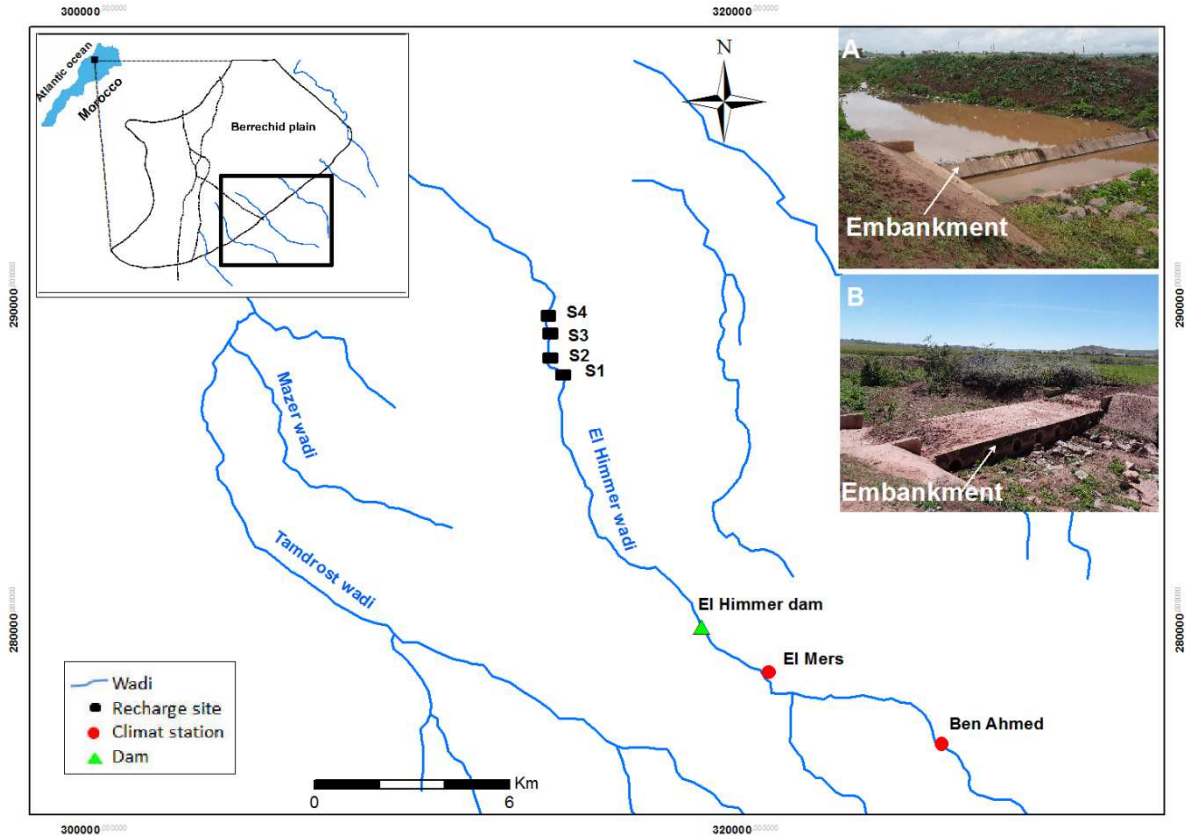


Fig.1. The study sites (S1, S2, S3, and S4) are located along the El Himmer Wadi. Inset photos indicate a (A) Percolation Tank and (B) a Recharge releases located at the studied sites (S1 and S2)

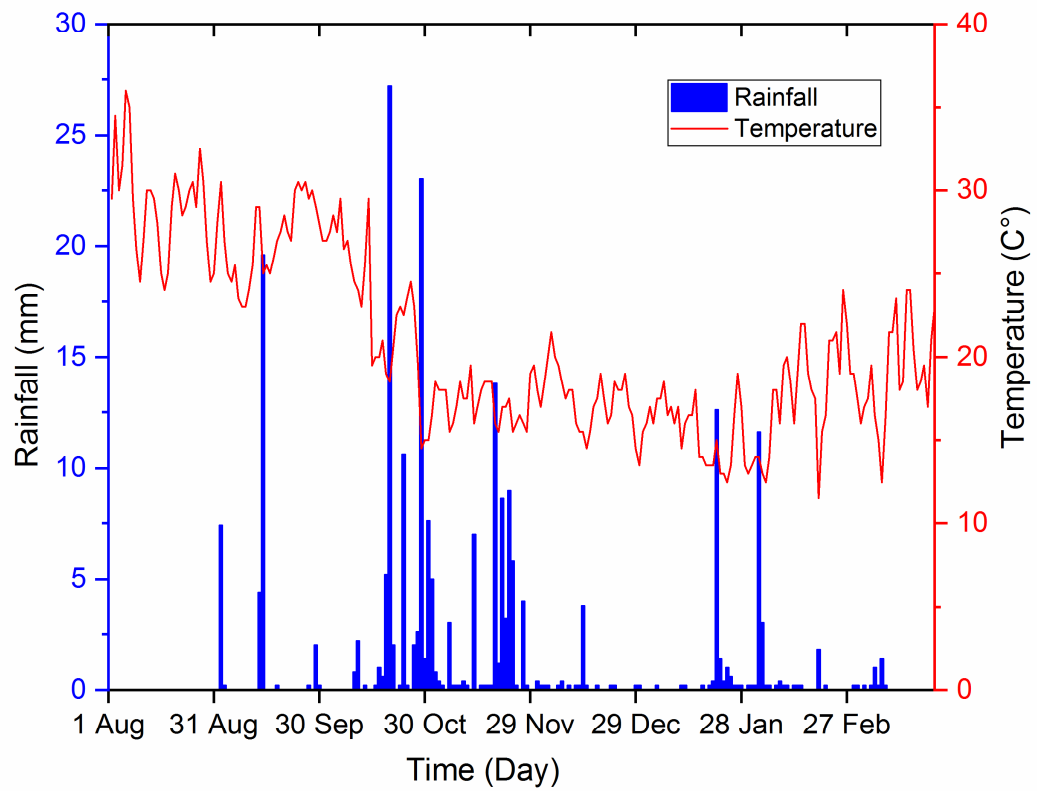


Fig.2. Daily rainfall and temperature at El Mers climate station in El Himmer wadi from 01/08/2018 to 24/03/2019

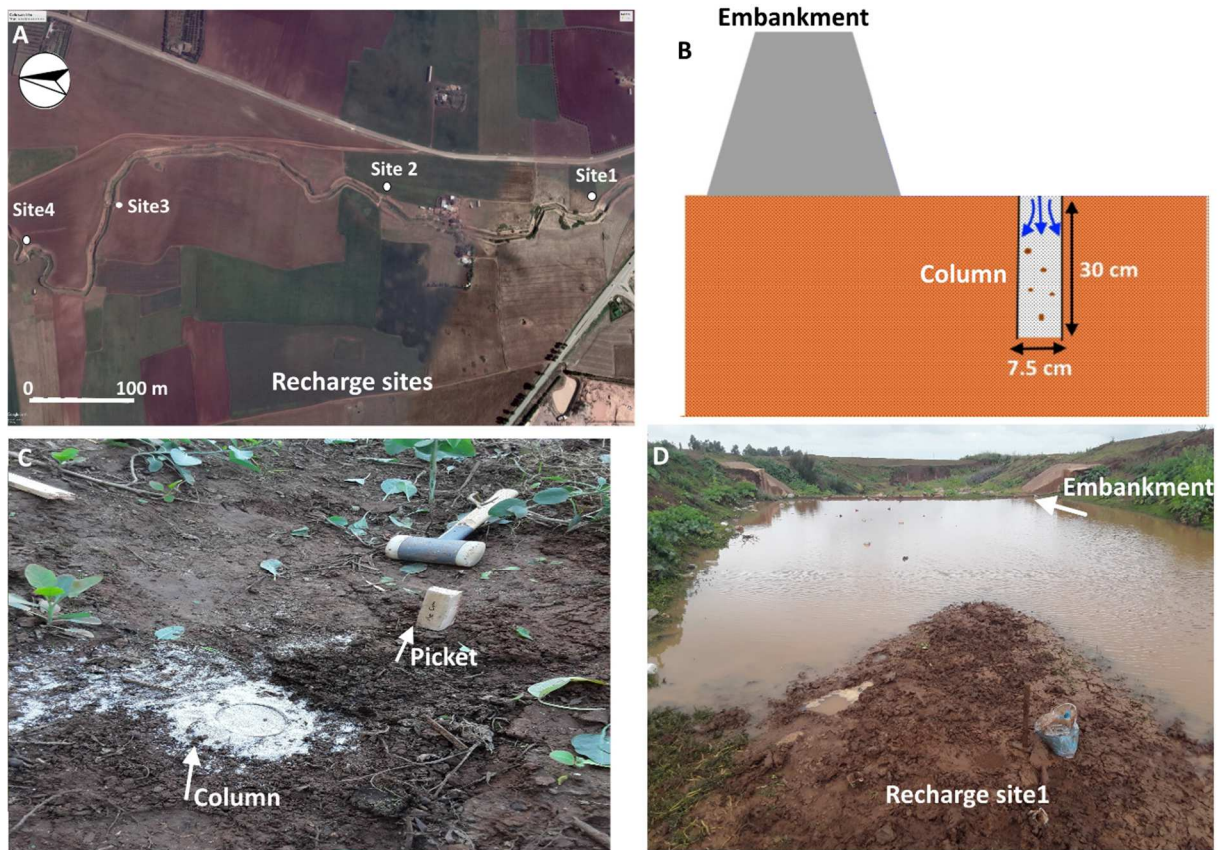


Fig.3. Layout at the field site. The upper panels show recharge sites positions in El Himmer wadi (A) and not scaled schematic profile of the columns implating on the wadi bed (B). The lower panels show photo of filling column and picket installed before runoff (C) and recharge site during high-flow (D)

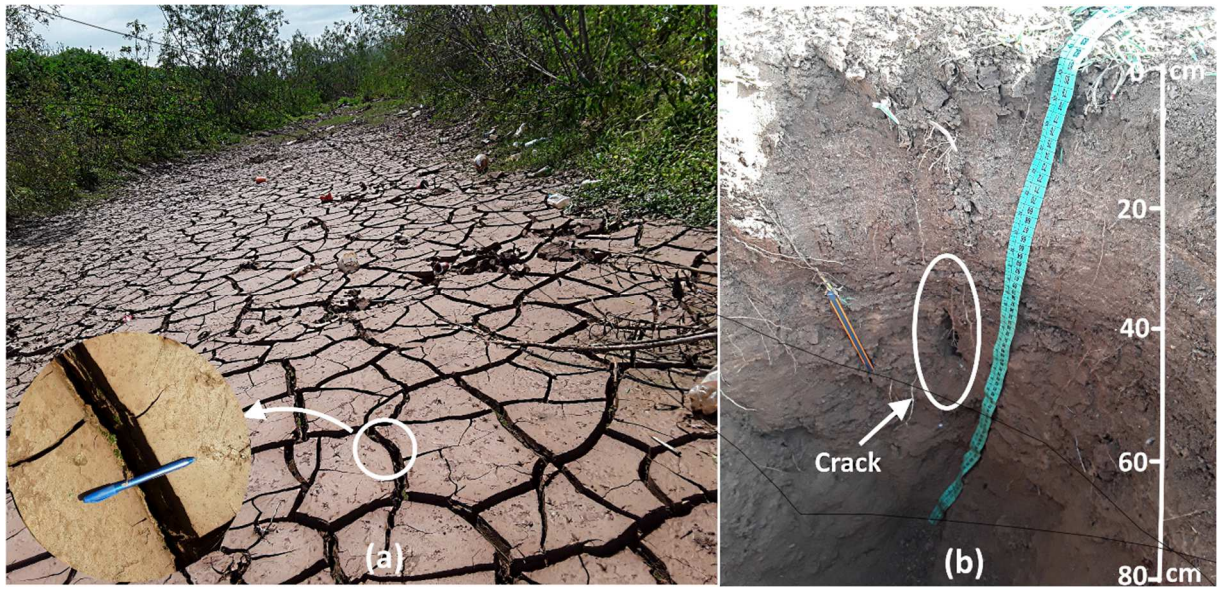


Fig.4. Photo of the surface (a) and (b) subsurface cracks in the field study in dry period

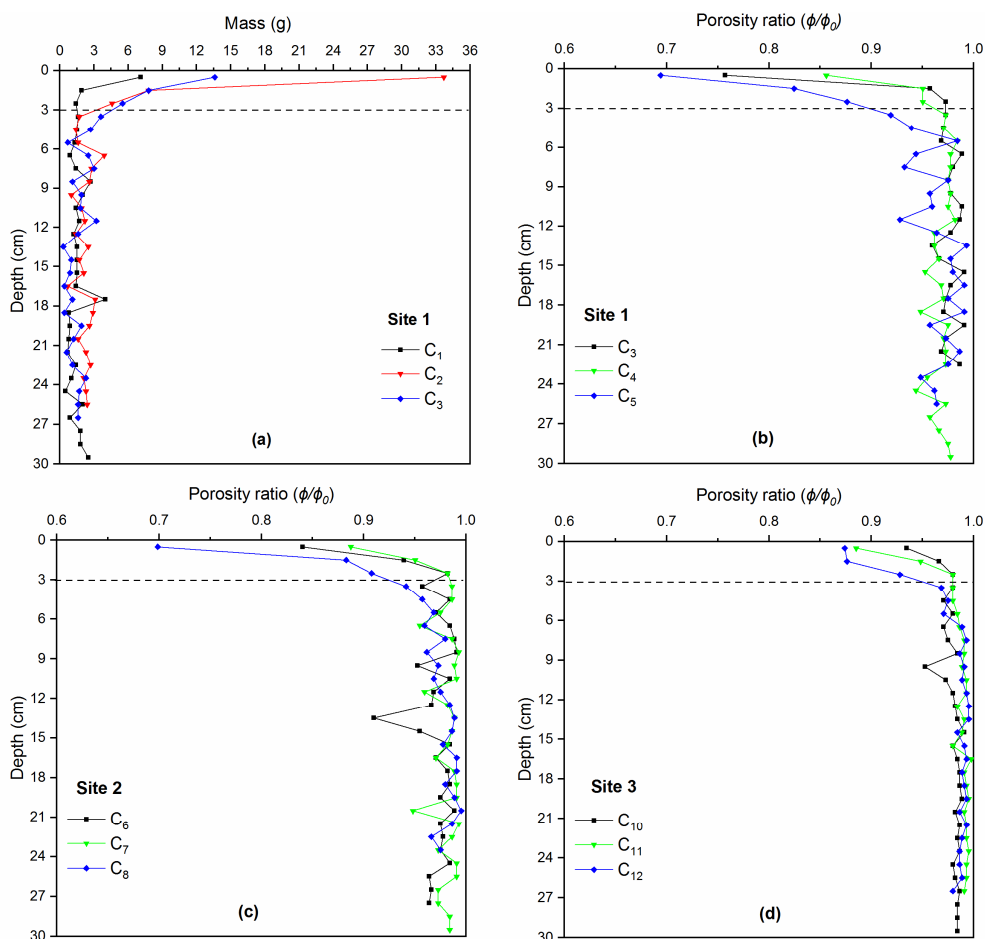


Fig.5. (a) Mass of the retained particles in the sand filled columns C1, C2, and C5 implanted in site S1. Profiles of porosity decline of the clogged sand filled columns implanted in sites (b) S1, (c) S2, and (d) S3

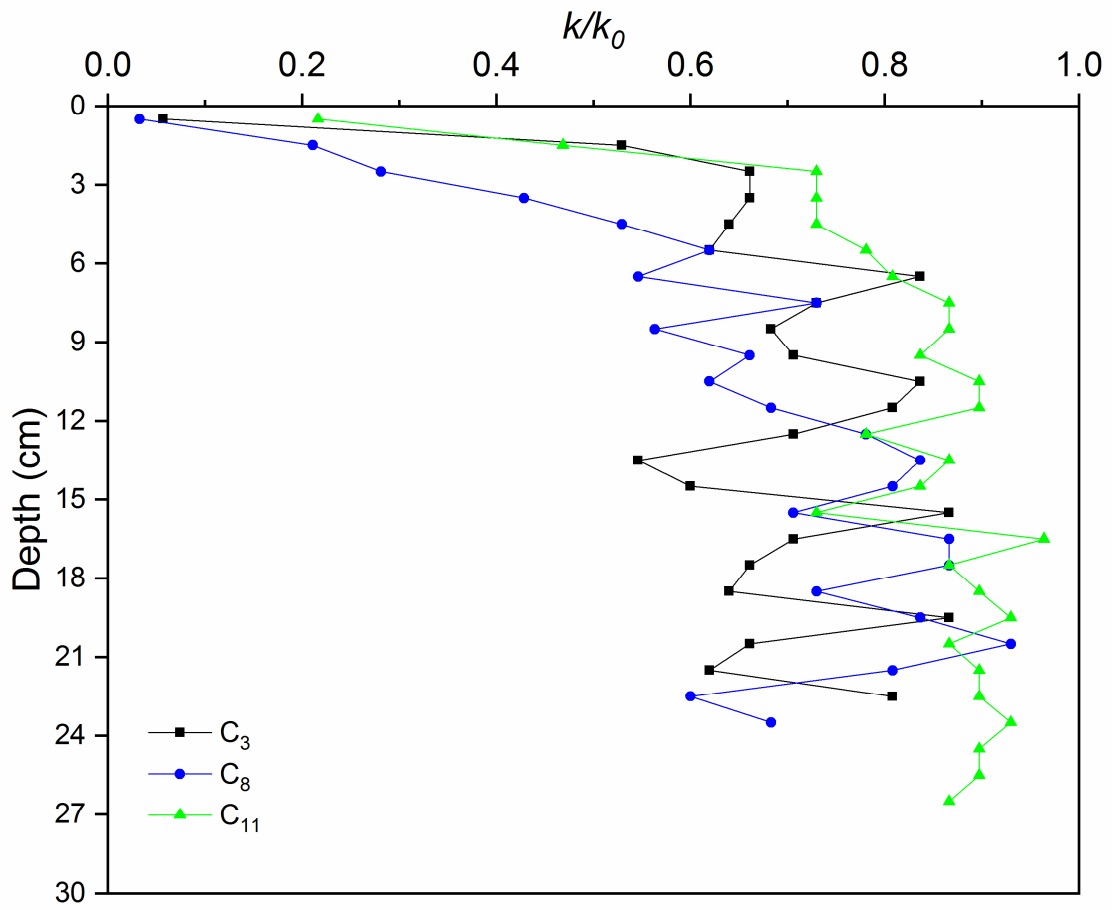


Fig.6. Hydraulic conductivity ratio of the sand filled columns C3, C8 and C11 from sites S1, S2 and S3 respectively

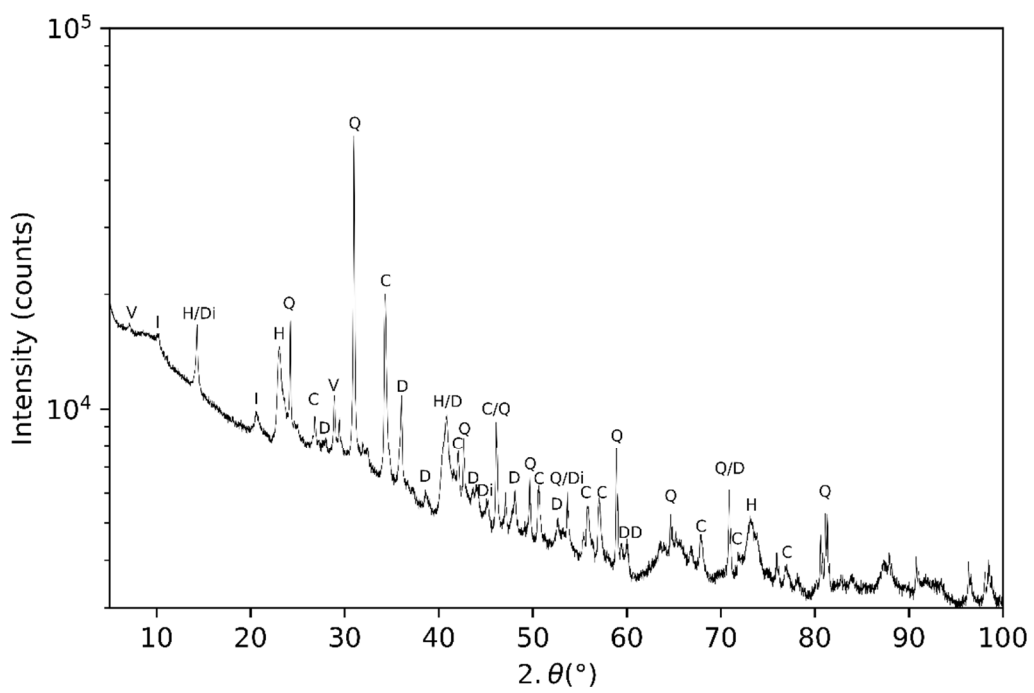


Fig.7. Powder diffraction of the mineral indicating the presence of vermiculite (V), interstratified illite-vermiculite (I), halloysite (H), dickite (Di), dolomite (D), quartz (Q) and calcite (C). Some peaks were not indexed in order to avoid redundancy

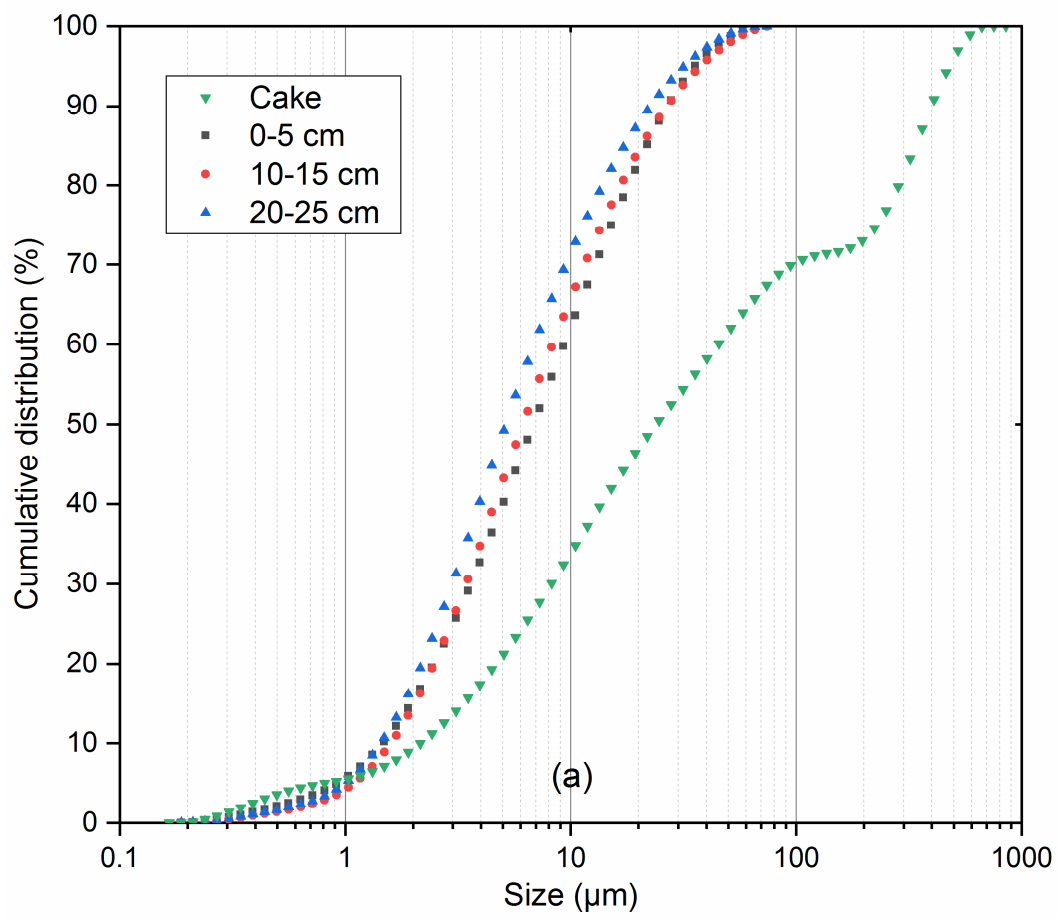


Fig.8. Particle size distribution of the particles retained in surface (cake) and subsurface (internal deposition) of the columns implanted in wadi bed

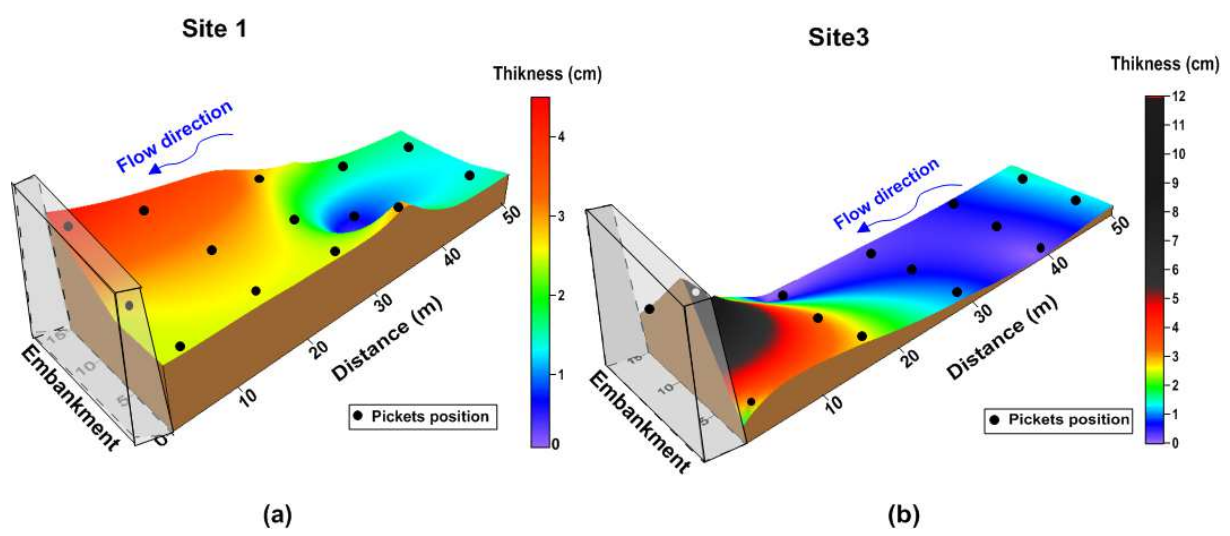


Fig.9. Thickness of surface deposits in the recharge a) site S1, and b) site S3

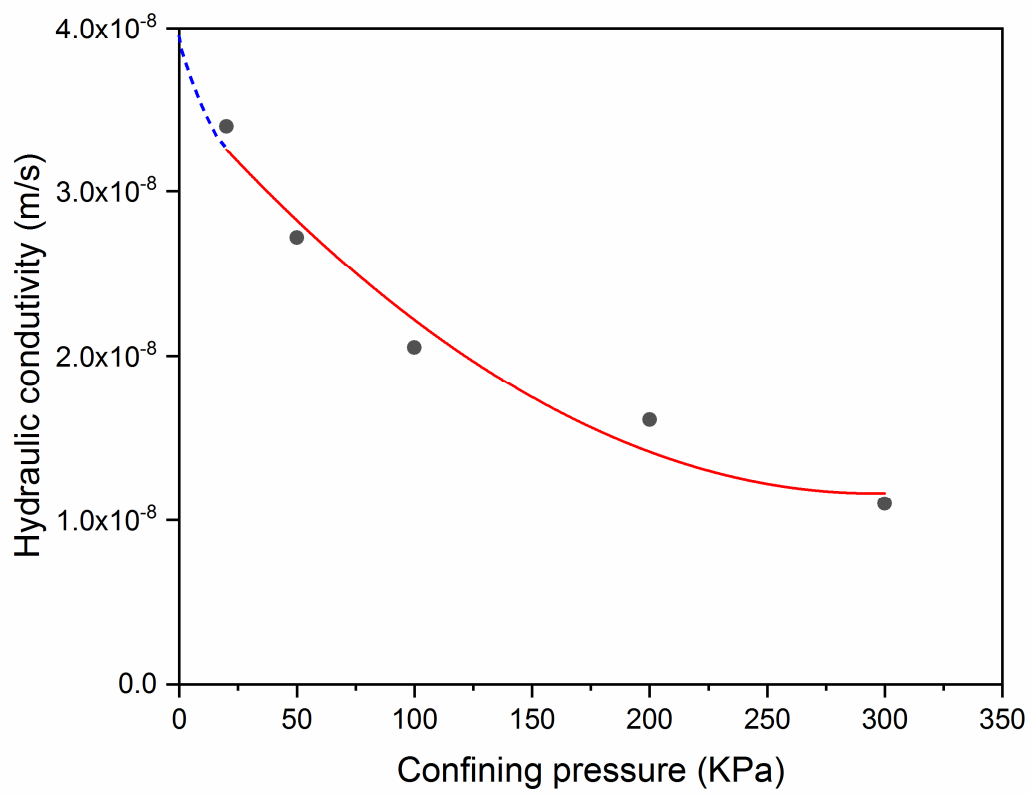


Fig.10. Example of measurement of the hydraulic conductivity for a formed cake (3.5 cm diameter and 3 cm high) at different confining pressures

Tables

Table 1. Mass of deposits in sand filled columns in the first 3 cm and between 3 and 30 cm depth

		Site S1					Site S2				Site S3		
Column number		C ₁	C ₂	C ₃	C ₄	C ₅	C ₆	C ₇	C ₈	C ₉	C ₁₀	C ₁₁	C ₁₂
Deposit Mass (g)	0 - 3 cm	10.4	46.1	13.9	10.8	26.9	10.6	8.0	22.7	18.3	5.3	8.3	14.3
	3 - 30 cm	51.1	95.6	34.2	48.0	65.1	41.5	30.2	45.1	65.3	28.0	19.0	27.7

Table2. Thickness of the deposited particles (cake) on columns surfaces

	S1					S2				S3		
Column	C ₁	C ₂	C ₃	C ₄	C ₅	C ₆	C ₇	C ₈	C ₉	C ₁₀	C ₁₁	C ₁₂
Cake thickness (cm)	4.0	2.5	0.7	0.5	2.0	3.0	3.0	0.5	0.5	7.0	2.8	0.0

Table 3. Size of the particles retained in depth and in surface (cake)

	$(\leq 63 \mu\text{m}) (\%)$	$(> 63 \mu\text{m})(\%)$	$d_{P10}(\mu\text{m})$	$d_{P50}(\mu\text{m})$	$d_{P90}(\mu\text{m})$
Particles retained in surface	66.0	34.0	2.1	24.7	409.0
Particles retained in depth	100.0	0.0	1.5	6.0	25.0

